AT&T Technical Journal
Vol. 64, No. 4, April 1985
Printed in U.S.A.

A Simulation Study of Space Diversity and Adaptive Equalization in Microwave Digital Radio

By L. J. GREENSTEIN and Y. S. YEH*

(Manuscript received May 30, 1984)

In this paper we analyze the performance of M-level quadrature amplitude modulation digital radio systems subjected to microwave multipath fading. We consider two kinds of adaptive receiver techniques, either singly or in combination: dual space diversity and adaptive equalization. The space diversity is assumed to be of either the selection type or the continuous-combining type, and the equalization is assumed to be ideal. We describe a specific form of combining which is optimal when no post-combiner equalization is used. A primary aim of the study is to quantify the performance of this combining approach and to compare it with alternate strategies. The study uses Monte Carlo simulations of the dual-channel fading response functions based on a recently published statistical model. For each response pair generated, a receiver detection measure is derived analytically in terms of the system parameters and receiver approach. Probability distributions of this measure, obtained by simulating several thousand response pairs, are then computed. They can be interpreted as displaying the link outage probability as a function of the number of modulation levels (M). We find that the appropriate combining scheme can serve in some cases to avoid the need for adaptive equalization. Also, where post-combiner equalization *is* used, the same scheme, while no longer optimal, can sharply reduce the dispersion seen by the equalizer input.

I. INTRODUCTION

A continuing challenge in microwave digital radio is to find ways to counter multipath fading. Many recent efforts—theoretical, experi-

* Authors are employees of AT&T Bell Laboratories.

mental, and developmental—have addressed the use of space diversity and adaptive equalization, individually or in combination, to maintain stringent outage objectives for increasingly high-level modulations.[1–14] This paper reports on a comparative study of several receiver processing approaches, enlarging on the evaluations presented in a companion paper.[15]

The receiver processing approaches studied here consist of three space diversity options, namely, *no* diversity, *selection* diversity, and *continuous-combining* (or *combining*) diversity. For each of these options, we evaluate performance statistics both *with* and *without* the presence of ideal adaptive equalization.

Our investigation is facilitated by a new statistical model for the response functions of two space diversity channels.[16,17] We describe that model in Section II and introduce some extensions germane to the present study.

We assume throughout this work a system using M-level Quadrature Amplitude Modulation (M-QAM) with cosine roll-off spectral shaping. This system and the various space diversity/equalization configurations to be studied are described in Section III.

For any given dual-channel response pair and receiver processing approach, we can compute one or more relevant performance measures. By combining the published model with Monte Carlo simulation techniques to generate response pairs, we can obtain probability distributions of these measures over an ensemble of multipath fades. In Section IV we define the performance measures to be studied and outline the analytical methods by which they are computed, and in Section V we describe the method of Monte Carlo simulation and present quantitative results. These are in the form of probability distributions and reveal the influence of various system parameters, channel parameters, and receiver processing approaches on link performance.

II. DUAL-CHANNEL FADING MODEL

2.1 Background

We are dealing with propagation media and systems wherein the multipath delay spread generally is small compared to the inverse channel bandwidth. Consequently, fading responses vary smoothly with frequency over a given channel and can be accurately approximated using simple functions. A popular complex function for this purpose is the one introduced by Rummler, initially for nondiversity channels[18,19] and, more recently, for dual-diversity channels.[16,17] In its most general form, Rummler's function approximates a complex response $H(f)$ on a given frequency interval, $[-W/2, W/2]$, with $W \leq 40$ MHz, by

$$\tilde{H}(f) = [c_1 + c_2 e^{-j\omega\tau}]e^{-j\omega t_o}; \qquad |f| \leq W/2, \qquad (1)^*$$

where c_1 and c_2 are complex coefficients that vary slowly with time but can be regarded as quasistatic; τ is a fixed parameter (6.3 ns); and t_o is a time delay (nominally, the propagation delay through the medium for which $H(f)$ is the response). If $H(f)$ were precisely known on $[-W/2, W/2]$, $\tilde{H}(f)$ could be fitted to it by first choosing least-mean-squared values for c_1 and c_2 (i.e., by minimizing, for given t_o, the integration of $|H(f) - \tilde{H}(f)|^2$ over $[-W/2, W/2]$), and then minimizing the result with respect to t_o.

An alternate form for $\tilde{H}(f)$ that more closely resembles the form used by Rummler is

$$\tilde{H}(f) = a[1 - be^{-j\omega\tau}]e^{j(\Phi_o - \omega t_o')}; \qquad |f| \leq W/2, \qquad (2)$$

where a is real and positive; b is complex; $|b| \leq 1$; and τ is either +6.3 ns ("minimum-phase" response) or −6.3 ns ("nonminimum-phase" response). For each of these two conditions, it is a simple matter to relate a, b, Φ_o, and t_o' to c_1, c_2, and t_o in (1). The question "minimum phase or nonminimum phase" has been left open to date, since only amplitude versus frequency data have informed the major attempts at statistical modeling.[18–20]

In Rummler's work, the phase factor $\exp(j(\Phi_o - \omega t_o'))$ is omitted. Again, this is necessitated by the absence of phase versus frequency information in the available databases. In nondiversity reception, moreover, this factor is immaterial since the phase Φ_o and time delay t_o' would be tracked, and their effects removed, by the carrier and timing recovery circuits of the receiver.

Now, however, consider the dual-diversity case. As before, each of the two responses, $H_1(f)$ and $H_2(f)$, can be approximated on $[-W/2, W/2]$ using functions like (1) or (2). Since combining diversity involves forming the composite response $\beta_1 H_1(f) + \beta_2 H_2(f)$, the Φ_o term for each channel is immaterial; these phases can be regarded as absorbed into the phases of β_1 and β_2. The difference in t_o' for the two channels, however, is another matter. We will return to this point later, after we summarize the statistical model.

2.2 Joint statistics: Rummler's model

The dual-diversity model is derived from data collected on a 26.4-mile path in Georgia in the 6-GHz band. The details—data, methods, and results—are well documented in Refs. 16 and 17. Here we will merely state some major results, using slightly different symbols where appropriate.

* Throughout this work, f is frequency measured from the center of the RF or IF channel under study, so that all responses are equivalent low-pass functions.

To begin with, the expected number of fading seconds on a microwave hop per year is

$$T_o = 52{,}800c(F/6)(D/25)^3, \tag{3}$$

where F is the microwave carrier frequency in GHz; D is the hop length in miles; and c is the terrain factor, varying between 0.25 and 4. During the rest of the year (normal propagation), the two response functions are $H_1(f) = H_2(f) = 1 + j0$. During multipath fading, however, they are

$$H_1(f) = a_1[1 - b_1\exp(\pm j\omega\tau)], \tag{4a}$$

$$H_2(f) = a_2[1 - b_2\exp(\pm j\omega\tau)], \tag{4b}$$

where $\tau = 6.3$ ns and the proper sign to use before it is an open question. Both functions apply over the limited range $|f| \leq W/2$, where $W \leq 40$ MHz.

The joint statistics of the a's and b's in (4) were published initially in Ref. 16. To smooth out some apparent artifacts of the data collections and reductions, Rummler subsequently published a "rationalized" version in Ref. 17. We will not reproduce his mathematical descriptions for the joint statistics, but a few important features should be noted:

- The four quantities $|b_1|$, $\text{Arg}\{b_1\}$, $|b_2|$ and $\text{Arg}\{b_2\}$ are mutually independent random variables, which means that the relative shapes of $H_1(f)$ and $H_2(f)$ are statistically independent.
- The amplitude factors a_1 and a_2 are lognormal random variables, i.e., their decibel values are Gaussian. Moreover, the mean of each Gaussian variable is a function of the magnitude of the corresponding b; each of the variations about the mean has a standard deviation near 7.0 dB; and the two variations are correlated.
- For the data reductions reported in Ref. 16, the correlation factor (ρ) between these variations was 0.65. In Ref. 17, Rummler generalizes this result by giving a simple empirical relationship between ρ and the vertical spacing of the diversity antennas.

2.3 Extensions and sensitivity considerations

We have modified Rummler's model, for purposes of our study, in three ways. First, we address the minimum-phase/nonminimum-phase question in the following manner: Let

$$H_1(f) = \begin{cases} a_1[1 - b_1e^{-j\omega\tau}] & \text{with probability } p \\ a_1[b_1 - e^{-j\omega\tau}] & \text{with probability } (1 - p). \end{cases} \tag{5}$$

Assuming that $\tau = 6.3$ ns and $|b| \leq 1$, we see that the first form is minimum phase and the second form is nonminimum phase. Thus, p

is the fraction of fades for which the form of $H_1(f)$ is minimum phase. We use the same description for $H_2(f)$, and assume that the minimum-phase condition occurs independently for the two response functions. In our simulations, we treat p as a parameter and vary it from 0 to 1 to assess its importance.

Second, we assume that $H_2(f)$ contains an additional phase factor, $\exp(-j\omega\delta t)$, where δt is the difference in t_o' for the "best" approximations to the two channel responses. This quantity cannot be known without simultaneous coherent measurements on both channels. We estimate, however, that it can be ±2 ns just from time delay misalignments between the two diversity branches. Allowing as much as ±4 ns for propagation differences, we speculate that δt lies between ±6 ns. We parameterize it accordingly in our simulations, always holding it fixed for a given run of Monte Carlo trials.

Finally, we allow the possibility that the correlation factor (ρ) between the decibel variations of a_1 and a_2 can differ from one path or time period to another, even for the same antenna spacing. We treat it parametrically in our simulations, varying it from 0 to 1 to assess its importance.

To summarize, we are concerned that our simulation results be "robust", i.e., not sensitive to—or artifacts of—uncertain features of the model. For this reason, we have identified some key uncertainties, cast them in terms of numerical quantities (p, δt, and ρ), and treated these quantities as parameters. As for the joint statistics assumed for the a's and b's in (4),[16,17] it is conjectural whether these descriptions would be applicable to all paths and time periods. For now, we regard these statistics as representative and useful for study purposes.

III. RECEIVER PROCESSING APPROACHES

3.1 General receiver structure

All the receiver processing approaches to be considered here can be cast as special cases of the general arrangement in Fig. 1. The original transmission is an M-QAM signal whose baseband pulse has the Fourier transform $\sqrt{C(f)}$, with $C(f)$ being the cosine roll-off function.[21] The two receiver inputs differ only in that the propagation medium delivers a different response into each space diversity antenna. Typically, the antennas would be vertically displaced by 40 feet or more so as to receive relatively uncorrelated responses during fading. Each diversity branch is shown having a separate, adaptable complex gain. The space diversity combiner is terminated by a signal adder that delivers a single-branch signal to the remainder of the receiver. Although shown here at RF, this circuitry could as readily be at IF. Also (though not made explicit by the figure), we assume there is

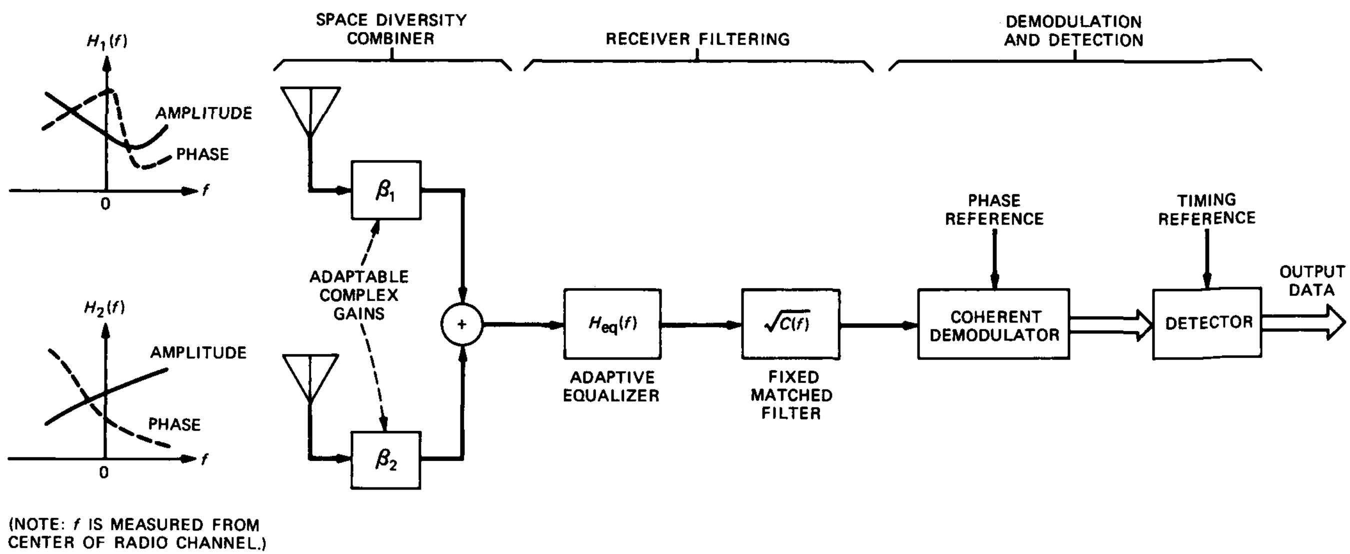

Fig. 1—Block diagram of a digital radio receiver with dual-channel space diversity. The modulation is M-QAM and the spectral shaping is cosine roll-off.

sufficient front-end amplification that the combiner gains β_1 and β_2 have no effect on receiver noise figure.

The combiner output is shown applied to an adaptive equalizer, with response $H_{eq}(f)$. For the cases studied that do not involve the use of equalization, we will set $H_{eq}(f)$ to unity. The second post-combiner filter has a fixed response, $\sqrt{C(f)}$, which provides matched filter reception in the absence of fading. Because the receiver is linear, the order of the adaptive and fixed filters is immaterial, as is the manner in which each is distributed among RF, IF, and baseband stages.

The coherent demodulation stage uses a quadrature pair of local oscillator signals which we assume to be optimally phased.* The baseband outputs are sampled in the detector every T seconds, where T is the symbol period ($1/T$ is the baud), and we assume the sampling phase (timing epoch) to be optimal.

What is *not* shown in Fig. 1 is the means for controlling the adaptable gains, i.e., the tap gains of the equalizer (if used) and the diversity branch gains, β_1 and β_2. Regarding the former, adaptive equalization is a well-developed art, and so we shall merely assume idealized equalizer responses, confident that they can be closely realized in practice. Regarding the latter, we shall specify idealized criteria for determining β_1 and β_2, both for selection diversity and combining diversity, and shall apply these criteria analytically in our performance calculations. Only in the case of combining diversity, however, will we address the issue of practical implementation.

3.2 Space diversity options

We delineate the three particular diversity options as follows:

1. *Nondiversity*, wherein only the response $H_1(f)$ (corresponding to the higher antenna) is received; thus, $(\beta_1, \beta_2) = (1, 0)$.

2. *Selection diversity*, wherein (β_1, β_2) is either (1, 0) or (0, 1), i.e., only one branch is processed at a given time, depending on which is deemed "best" in some sense.

3. *Combining diversity*, wherein β_1 and β_2 are continuously variable and are adjusted according to a specified criterion.

We will discuss these options first for the case of no adaptive equalization ($H_{eq}(f) = 1 + j0$ in Fig. 1). Accordingly, the composite channel response as seen at the fixed filter input is

$$H(f) = \beta_1 H_1(f) + \beta_2 H_2(f), \tag{6}$$

where all quantities are complex.

The nondiversity case is included here for purposes of comparison.

* Optimal carrier and timing phase is meant, in these discussions, to denote phases for which the detection signal-to-distortion ratio is maximal.

It will be shown to yield disastrous performance results in the absence of equalization, as expected.

For the case of selection diversity, the signal adder would, in practice, be a selection switch operated by real-time decisions of some kind. We will obtain results for a theoretically optimal selection strategy, described as follows: At all times, (β_1, β_2) is either (1, 0) or (0, 1), whichever yields the lower bit error rate for the prevailing response pair, $(H_1(f), H_2(f))$. Since selection diversity is included here primarily for purposes of comparison, we ignore the issue of practical implementation.

The combining diversity case is the one that interests us most. We will show that combining diversity alone (i.e., without equalization) can go a long way towards combatting dispersion as well as noise. As explained in Ref. 15, this potential exists for any channel over whose bandwidth the frequency response can be approximated by a first-order polynomial in $j\omega$. This condition applies to the microwave common-carrier channels at hand.[20]

The criterion we will assume for adapting (β_1, β_2) in the absence of equalization is maximization of a particular signal-to-distortion ratio at the detector, where "distortion" includes Intersymbol Interference (ISI) and noise. This ratio, which we call ρ_D, is defined and analyzed in Section 4.1. We will see that ρ_D is quadratic in β_1 and β_2; thus, a unique maximum exists and the (β_1, β_2) pair that produces it can be found analytically. More important, it is well known that this solution for (β_1, β_2) can be realized in a receiver by means of practical circuitry, specifically, via decision-directed gradient search algorithms.[22,23]

In Ref. 15 we describe an alternative scheme for adapting (β_1, β_2) that does *not* rely on data decisions and yet produces results close to those using the more conventional approach. The scheme involves measuring the combiner output power spectrum density at three or more inband frequencies, computing from these samples a measure that approximates ρ_D, and using this measure to drive the search over β_1 and β_2.

With all this in mind, we will derive analytical solutions for the (β_1, β_2) pair that maximizes ρ_D in the absence of equalization, and will denote it by $(\tilde{\beta}_1, \tilde{\beta}_2)$. Since maximizing ρ_D minimizes an upper bound on the bit error rate (Section 4.1), we will call this gain pair *optimal*. Finally, we will assume that optimal or near-optimal solutions can always be realized in practical receivers using schemes such as those mentioned above.

3.3 Receivers with adaptive equalizers

A variety of practical approaches could be assumed for the equalizer in Fig. 1. These include the reciprocal equalizer,[24] the Minimum Mean

Square Error (MMSE) equalizer,[25] the Decision Feedback Equalizer (DFE),[26] and adaptive cancellation.[27] In terms of detection signal-to-distortion ratio, these four approaches improve in the order cited. However, in terms of outage performance over a large ensemble of fading responses, there seems to be little to differentiate among them.[28,29] We shall therefore assume an ideal reciprocal equalizer, both because it is the easiest to analyze and because it provides a tight worst-case bound on the performance of the more optimal equalizers.

The reciprocal equalizer has a response

$$H_{eq}(f) = \frac{1}{H(f)} = \frac{1}{\beta_1 H_1(f) + \beta_2 H_2(f)}. \tag{7}$$

Its obvious effect is to restore the received signal to what it would have been without multipath fading and space diversity. In the process, it eliminates ISI but produces a noise enhancement proportional to the integral of $C(f)/|H(f)|^2$ (see Fig. 1), where $C(f)$ is the cosine roll-off function. We will analyze this equalizer in conjunction with the three space diversity options (nondiversity, selection diversity, and combining diversity) discussed in Section 3.2.

In evaluating selection diversity with equalization, we will again assume a theoretically optimum strategy: At all times, $(\beta_1, \beta_2) = (1, 0)$ or $(0, 1)$, whichever yields the lower bit error rate for the prevailing response pair, $(H_1(f), H_2(f))$. As before, we will not consider the issue of practical implementation.

In evaluating combining diversity with equalization, we will consider three practical strategies for adapting β_1 and β_2. They are as follows:

1. The relative amplitude and phase of β_1 and β_2 are adjusted to maximize the ratio of signal power to noise power at the combiner output.

2. Only the relative phase of β_1 and β_2 is adjusted to maximize the same ratio, with $|\beta_1| = |\beta_2| = 1$.

3. β_1 and β_2 are adjusted to those values, $\tilde{\beta}_1$ and $\tilde{\beta}_2$, that would maximize ρ_D *in the absence of equalization.*

Missing from this list of strategies is the (β_1, β_2) pair that maximizes ρ_D in the *presence* of equalization. Unfortunately, the analytical solution for this case is somewhat intractable. Also, its realization in practice would probably require using data decisions, which might be unreliable when recovering from severe fades. Each of the above three strategies, by contrast, could be implemented using simple power measurements at the combiner output. The first two would involve a single, full-channel power measurement to drive the search over β_1 and β_2, while the third would involve three or more inband power spectrum density measurements, as described in Ref. 15.

We emphasize that the third strategy is not optimal in the presence of equalization. Indeed, both of the first two strategies will be shown to yield superior outage statistics. Nonetheless, we will continue to refer to the gain pair $(\tilde{\beta}_1, \tilde{\beta}_2)$ as optimal, but with quotation marks added. Thus, the gain pair $(\tilde{\beta}_1, \tilde{\beta}_2)$ is called optimal when there is no equalization and "optimal" when there is.

Why even consider the third strategy in the presence of equalization if it does not yield the best detection? Because it serves another beneficial purpose, namely, sharply limiting the signal dispersion as seen at the input to the equalizer. The virtue in doing this is that it simplifies the circuitry needed to approximate the performance of ideal adaptive equalizers. For example, a digital equalizer might require fewer taps and/or lesser quantizing resolution by operating on input signals with less dispersion. Moreover, Gersho has shown that equalizer convergence speed improves as input signal dispersion decreases.[30]

Table I summarizes this section by giving, for each combination of space diversity and equalization to be considered, the assumed criteria for adapting (β_1, β_2).

IV. ANALYSIS

4.1 Receiver detection measure

In current digital radio systems, the symbol rate $(1/T)$ is typically 75 percent of the channel bandwidth (W) and α is typically between 0.25 and 0.5. Our simulations will assume typical symbol rates but, for convenience, will show results for $\alpha = 0$. This case is especially easy to treat because the cosine roll-off function, $C(f)$, reduces to a rectangle on $[-1/2T, 1/2T]$ and this simplifies the analysis and computation of ISI power. At the same time, this approach leads to slightly

Table I—Criteria for adapting (β_1, β_2) under different space diversity/equalization approaches

	Equalization	
Space Diversity	None	Reciprocal Equalizer
None	$(\beta_1, \beta_2) = (1, 0)$	$(\beta_1, \beta_2) = (1, 0)$
Selection diversity	$(\beta_1, \beta_2) = (1, 0)$ or $(0, 1)$, whichever yields larger ρ_D	$(\beta_1, \beta_2) = (1, 0)$ or $(0, 1)$, whichever yields larger ρ_D
Combining diversity	*Optimal* solution:* $(\beta_1, \beta_2) = (\tilde{\beta}_1, \tilde{\beta}_2)$	1. $\beta_1 = 1 + j0$; $\lvert\beta_2\rvert$ and $\text{Arg}\{\beta_2\}$ set to maximize combiner output s/n 2. $\beta_1 = 1 + j0$; $\lvert\beta_2\rvert = 1$; $\text{Arg}\{\beta_2\}$ set to maximize combiner output s/n 3. "Optimal" solution:* $(\beta_1, \beta_2) = (\tilde{\beta}_1, \tilde{\beta}_2)$

* $(\tilde{\beta}_1, \tilde{\beta}_2)$ is that gain pair for which ρ_D is maximized when there is no equalization.

pessimistic results since, for given $1/T$, ISI distortion decreases somewhat with α.[29,31] Our assumption for α, then, will serve both to simplify the analysis/computations and to yield worst-case estimates of detection performance.

To begin, we define

$P_S \triangleq$ The squared signal sample (excluding ISI and noise) in either baseband stream when a data value of +1 or −1 is being detected;

$P_I, P_N \triangleq$ The mean square ISI and noise, respectively, associated with the periodic samples in either baseband stream;

and

$$\rho_D \triangleq P_S/(P_I + P_N). \tag{8}$$

The latter is the detection signal-to-distortion ratio and can be related to an upper bound on the bit error rate via[28]

$$\text{Bit Error Rate} \leqslant 2\exp(-\rho_D/2). \tag{9}$$

This upper bound is particularly conservative when ISI dominates because this distortion component is generally peak limited, in contrast to Gaussian noise.

We first consider a receiver with no adaptive equalization ($H_{eq}(f) = 1 + j0$, in Fig. 1). For $\alpha = 0$, ρ_D can be shown to be

$$\rho_D = \frac{3}{M-1} \cdot \left\{ \frac{\underset{t_s}{\mathrm{Max}}(|\bar{H}|^2)}{[\overline{|H|^2} - \underset{t_s}{\mathrm{Max}}(|\bar{H}|^2)] + (|\beta_1|^2 + |\beta_2|^2)/\mathrm{CNR}} \right\} \text{(No Equalizer)}, \tag{10}$$

where*

$$\bar{H} = \int H(f)e^{j\omega t_s}df T; \tag{11}$$

$$\overline{|H|^2} = \int |H(f)|^2 df T; \tag{12}$$

CNR is the unfaded carrier-to-noise ratio per diversity branch in a bandwidth $1/T$ (typically close to 10^6, or 60 dB); $H(f)$ is given by (1); and t_s is the timing epoch. We assume the latter to be optimal, i.e., that value for which ρ_D is maximized. This assumption is implicit in (10), where t_s is specified to maximize $|\bar{H}|^2$.

* In this analysis, all integrals have limits $-1/2T$ and $1/2T$. For convenience, we omit them from the equations.

As for $\bar{H}$, it represents a complex gain for the signal vector sampled in each data interval. The imaginary part represents interference into each baseband rail from the cross-rail data in the same interval. Optimal carrier recovery amounts to multiplying $\bar{H}$ by a phase factor, $e^{j\theta}$, that makes it real and thus eliminates this interference. The resulting θ is the optimal carrier phase and the resulting signal gain is $|\bar{H}|$, as used in (10). In the case of optimal combining diversity, the optimal θ is implicitly realized in the course of optimizing β_1 and β_2. For both nondiversity and selection diversity, we will *assume* an optimal carrier phase without specifying how it is achieved.

Now we consider a receiver with an ideal reciprocal equalizer. The signal-restoring property of this equalizer is such that only thermal noise enhancement modifies ρ_D from its unfaded value. Thus, for the assumed system,

$$\rho_D = \frac{3}{M-1}\left\{\frac{\text{CNR}}{(|\beta_1|^2 + |\beta_2|^2)\displaystyle\int \frac{dfT}{|H(f)|^2}}\right\} \text{(Reciprocal Equalizer).} \tag{13}$$

The receiver detection measure we will use, and for which we will find probability distributions, is the bracketed quantity in (10) or (13). Thus, we define

$$\Gamma \triangleq \left(\frac{M-1}{3}\right)\rho_D, \tag{14}$$

which can be viewed as a normalized signal-to-distortion ratio. It is a function solely of the response pair $(H_1(f), H_2(f))$; the gain pair (β_1, β_2); and the system parameters T and CNR. Combining (14) with (9), we can upperbound the Γ required in an M-level system to achieve a specified bit error rate, BER_o:

$$\Gamma_o = \frac{2}{-}(M-1)\ln(2/\text{BER}_o). \tag{15}$$

Decibel values of Γ_o for various combinations of M and BER_o are given in Table II. We will use these values later in assessing the simulation results.

Table II—Decibel values of Γ_o for various M and BER_o

	M		
BER_o	16	64	256
10^{-3}	18.81	25.04	31.11
10^{-4}	19.96	26.19	32.26
10^{-5}	20.87	27.10	33.17
10^{-6}	21.62	27.85	33.92

4.2 Formulas for β_1 and β_2

We now present the appropriate gain pair (β_1, β_2) as a function of $(H_1(f), H_2(f))$ for each of the various receiver processing approaches.

In the cases of nondiversity and selection diversity, the specifications are simple: For both equalized and nonequalized receivers,

$$(\beta_1, \beta_2) = \begin{cases} (1, 0); & \text{(No Diversity)} \\ (1, 0) \text{ or } (0, 1), & \\ \text{whichever maximizes } \Gamma; & \text{(Selection Diversity).} \end{cases} \tag{16}$$

In the case of optimal combining diversity without equalization, the analysis is a bit complicated. The initial step is to rewrite (10) as

$$\rho_D = \frac{3}{M-1} \cdot \left\{ \underset{t_s}{\text{Max}} \left[\underset{(\beta_1,\beta_2)}{\text{Max}} \left\{ \frac{|\bar{H}|^2}{[\overline{|H|^2} - |\bar{H}|^2] + (|\beta_1|^2 + |\beta_2|^2)/\text{CNR}} \right\} \right] \right\}, \tag{10'}$$

where $\overline{|H|^2}$ and $|\bar{H}|^2$ are quadratic in β_1 and β_2 and $|\bar{H}|^2$ is, in addition, a function of t_s. The maximization over β_1 and β_2 can be done analytically using the method outlined in Ref. 25. Briefly, the denominator (quadratic in β_1 and β_2) is minimized subject to the constraint that $\bar{H}$ (linear in β_1 and β_2) equals $1 + j0$. This problem can be solved using Lagrange multipliers and leads to the following result:

$$\tilde{\beta}_1 = \text{NUM}_1/\Delta; \qquad \tilde{\beta}_2 = \text{NUM}_2/\Delta, \tag{17}$$

where

$$\text{NUM}_1 = \overline{H_1^* e^{j\omega t_s}} - \text{CNR}(\overline{H_2^* e^{j\omega t_s}}\ \overline{H_1^* H_2} - \overline{H_1^* e^{j\omega t_s}}\ \overline{|H_2|^2}); \tag{18}$$

$$\text{NUM}_2 = \overline{H_2^* e^{j\omega t_s}} - \text{CNR}(\overline{H_1^* e^{j\omega t_s}}\ \overline{H_1 H_2^*} - \overline{H_2^* e^{j\omega t_s}}\ \overline{|H_1|^2}); \tag{19}$$

$$\Delta = \text{NUM}_1 + \text{NUM}_2; \tag{20}$$

and $\overline{(\quad)}$ is the average over f from $-1/2T$ to $1/2T$. (Because the processing is linear, an equivalent form of the solution is $\tilde{\beta}_1 = 1 + j0$ and $\tilde{\beta}_2 = \text{NUM}_2/\text{NUM}_1$. For convenience only, we will use the solution as presented above.)

These solutions for $\tilde{\beta}_1$ and $\tilde{\beta}_2$ maximize ρ_D for a given value of t_s. In our computations, the above formulas were used to obtain the inner maximum in (10′), and then a numerical search over t_s was performed to find the outer maximum.

Finally, we consider the use of combining diversity *with* adaptive equalization. As noted in Section 3.3, three distinct strategies for adapting β_1 and β_2 have been considered. Mathematical formulas for β_1 and β_2 under these strategies are as follows:

1. $\beta_1 = 1 + j0$ and both the magnitude and phase of β_2 are adjusted to maximize the ratio of signal power to noise power at the combiner output. The solutions are

$$\text{Arg}\{\beta_2\} = \tan^{-1}[-\text{Im}(\overline{H_1^* H_2})/\text{Re}(\overline{H_1^* H_2})] \tag{21}$$

and

$$|\beta_2| = \frac{\gamma_a + \sqrt{\gamma_a^2 + 4\gamma_b}}{2\sqrt{\gamma_b}}, \tag{22}$$

where

$$\gamma_a = \overline{|H_2|^2} - \overline{|H_1|^2} \tag{23}$$

and

$$\gamma_b = [\text{Re}(\overline{H_1^* H_2})]^2 + [\text{Im}(\overline{H_1^* H_2})]^2. \tag{24}$$

2. $\beta_1 = 1 + j0$ and $|\beta_2| = 1$, with the phase of β_2 adjusted to maximize the same ratio. The solution for $\text{Arg}\{\beta_2\}$ is again (21).

3. $\beta_1 = \tilde{\beta}_1$ and $\beta_2 = \tilde{\beta}_2$, (17) through (20), where t_s is that timing epoch for which ρ_D in (10′) is globally maximized. (Again, $\beta_1 = 1 + j0$ and $\beta_2 = \tilde{\beta}_2/\tilde{\beta}_1$ would yield the same results.)

4.3 Channel outage probabilities

Our simulations lead to probability distributions for Γ over the ensemble of dual-channel response pairs. The probability distribution obtained for a given receiver technique will be denoted by $P(\Gamma)$, representing the expected fraction of multipath fading seconds for which the receiver detection measure lies below Γ. Thus, if Γ_o is the value that Γ must exceed for acceptable performance, then $P(\Gamma_o)$ is the conditional probability of channel outage (i.e., conditioned on the occurrence of fading). Further, if P_{req} is the maximum permissible value of that probability for meeting the system outage objective, the receiver technique can be considered adequate if and only if $P(\Gamma_o) \leq P_{req}$.

To apply this interpretation to our simulation results requires numerical data for both Γ_o and P_{req}. The former is derived in Section 4.1 and quantified, for various combinations of M and BER_o, in Table II. Derivations of P_{req} are outlined in the Appendix and quantified in Table III. These results are for short- and long-haul systems in the 4-, 6-, and 11-GHz bands, both with and without protection switching.

4.4 A performance measure for equalized receivers

A second performance measure for which we shall obtain probabil-

Table III—Values of P_{req} for various system conditions

Band	System Length	Protection Switching: None (Unprotected)	Protection Switching: One Protection Channel
4 GHz ($W = 20$ MHz)	Long haul	2.84×10^{-4}	6.88×10^{-3}
	Short haul	4.54×10^{-3}	2.75×10^{-2}
6 GHz ($W = 30$ MHz)	Long haul	1.89×10^{-4}	6.88×10^{-3}
	Short haul	3.03×10^{-3}	2.75×10^{-2}
11 GHz ($W = 40$ MHz)	Long haul	1.03×10^{-4}	5.87×10^{-3}
	Short haul	1.65×10^{-3}	2.35×10^{-2}

ity distributions is the *range* of $|H(f)|$ over the Nyquist bandwidth, $[-1/2T, 1/2T]$. Thus,*

$$R \triangleq \left\{\frac{\underset{f}{\text{Max}}|H(f)|}{\underset{f}{\text{Min}}|H(f)|}\right\}; \qquad |f| \leq 1/2T. \tag{25}$$

The quantity R is of interest in cases where adaptive equalization is used, for reasons given in Section 3.3. It is this index of input signal dispersion that has been shown to provide a measure of convergence speed.[30] We will see that its probability distribution, $P(R)$, depends strongly on diversity approach.

V. SIMULATION STUDY AND RESULTS

5.1 Simulation approach

A computer program was written that simulates response pairs $(H_1(f), H_2(f))$ in accordance with the statistical model discussed in Section II and, for each simulation trial, analyzes the receiver techniques described in Section III using the methods of Section IV.

The system parameters studied were channel bandwidth (W) and unfaded carrier-to-noise ratio (CNR). As discussed in Section 4.1, the symbol rate was taken to be 75 percent of the bandwidth (i.e., $1/T =$ 15, 22.5, and 30 megabaud, respectively, for $W = 20$, 30, and 40 MHz) and the cosine roll-off factor was taken to be zero. The values used for CNR ranged from 51 to 67 dB, with 63 dB taken to be the most "typical" value. The channel parameters studied were δt, p and ρ, as discussed in Section 3.4, with the "typical" values taken to be 4 ns, 0.5, and 0.65, respectively.

For each combination of receiver technique and parameter set, either or both of the quantities Γ and R were computed for each of four

* We use the Nyquist bandwidth in defining this measure, noting that it is the 6-dB bandwidth of the system response for *any* value of the cosine roll-off factor.

thousand response pairs. From the population of quantities obtained for each such "simulation run," we then computed the appropriate probability distribution(s), i.e., $P(\Gamma)$ and/or $P(R)$.

The response pair for each trial was obtained via Monte Carlo generation of the a's and b's in (4), according to the assumed model. The same set of four thousand response pairs was used in each simulation run, except for minor differences related to changed values for δt, p, and ρ. Our purpose was to permit comparisons among receiver techniques for the same fading channel ensemble.

We confirmed, in two ways, that the ensemble of four thousand response pairs generated suitably represents the model, namely, (1) by computing the ensemble statistics of a_1, a_2, $|b_1|$, $|b_2|$, etc., and comparing them with those predicted by the model; and (2) by computing $P(\Gamma)$ and $P(R)$ for several different sets of response pairs and examining the agreement between them. We thereby established that the simulations are accurate and consistent down to probability values of 0.005 or lower, which is sufficient for our purposes.

5.2 Results for combining diversity with no equalization

This is the receiver technique of greatest interest to this study, as we wish to determine the multipath-combatting potentialities of those routes equipped with space diversity antennas. We computed $P(\Gamma)$ for this case over a wide range of system and channel parameters.

5.2.1 System parameters: W and CNR

Figure 2 shows curves for $P(\Gamma)$ with W as a parameter. All other parameters are assumed to have "typical" values, i.e., CNR = 63 dB, $\delta t = 4$ ns, $p = 0.5$, and $\rho = 0.65$. The fairly strong influence of W is no surprise. The benefit gained by linearly combining $H_1(f)$ and $H_2(f)$ depends on how effectively this combining cancels their dispersive components. Cancellation is most readily achieved when these components are linear in $j\omega$ over the bandwidth, a condition most nearly approximated at smaller W.[15] As W increases, higher-order terms in $j\omega$ become prominent and a linear sum of two responses is less able to cancel the dispersions. In this light, we see that three or more diversity branches might yield significant gains at larger bandwidths.

To apply the results of Fig. 2 to a concrete example, we assume a protected short-haul 64-QAM system with a BER objective of 10^{-6}. Table II shows that $\Gamma_o \approx 28$ dB for this case, and Table III shows that $P(\Gamma_o)$ must lie below 0.0275, 0.0275, and 0.0235 for $W = 20$, 30, and 40 MHz, respectively. We thus see that using optimal combining diversity without equalization would suffice to meet outage objectives at 4, 6, and 11 GHz (the latter case being somewhat marginal). To meet *long-haul* objectives, however (see Table III), or to operate

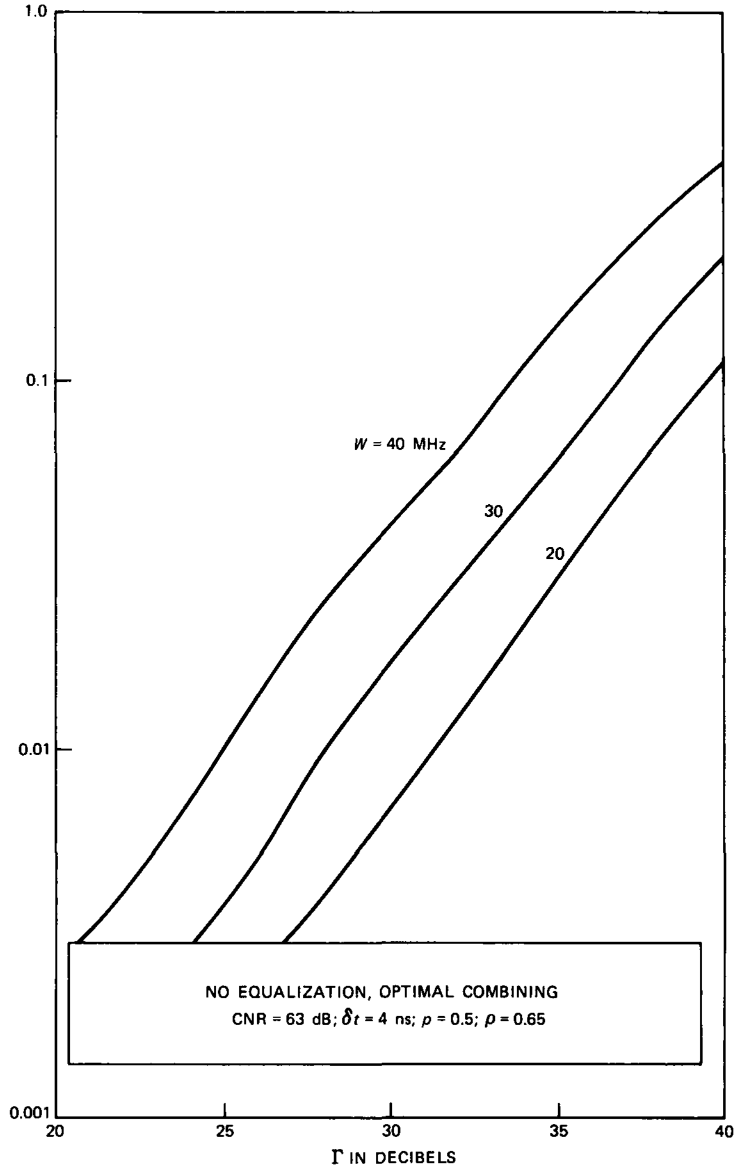

Fig. 2—Probability distributions for Γ in receivers with optimal diversity combining and no equalization. The parameter is channel bandwidth, W. All other system and channel parameters have "typical" values: CNR = 63 dB, δt = 4 ns, p = 0.5, and ρ = 0.65.

without protection switching or at 256 levels, optimal combining alone would be marginal or downright inadequate, at least for 6- and 11-GHz systems.

To study the influence of CNR, Fig. 3 shows $P(\Gamma)$ for $W = 30$ MHz

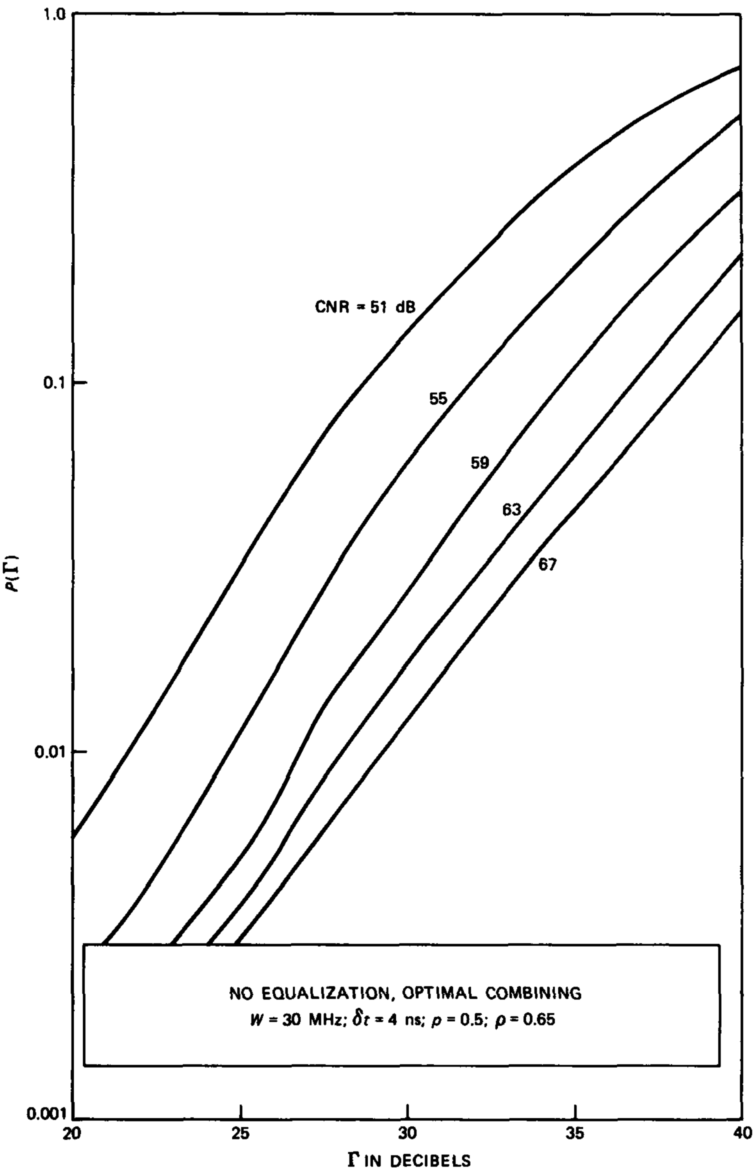

Fig. 3—Probability distributions for Γ in receivers with optimal diversity combining and no equalization. The parameter is CNR. Channel bandwidth $W = 30$ MHz, and all other system and channel parameters have "typical" values.

with CNR parameterized over the range from 51 to 67 dB. The trend is similar for all other W. The sensitivity of the results to CNR is seen to increase as this quantity decreases; this is because noise becomes an increasingly significant factor (as opposed to intersymbol interference) as CNR decreases.

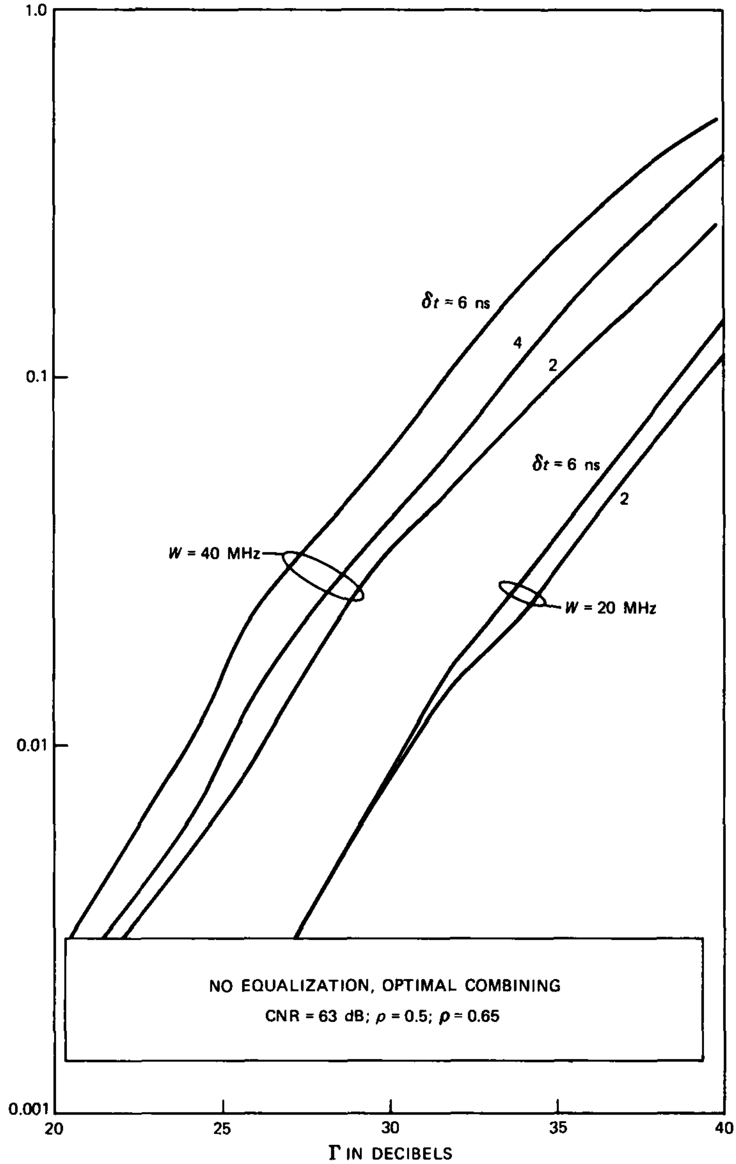

Fig. 4—Probability distributions for Γ in receivers with optimal diversity combining and no equalization. The primary parameter is δt, with results given for $W = 20$ and 40 MHz. All other system and channel parameters have "typical" values.

5.2.2 Channel parameters: δt, p, and ρ

Figure 4 shows $P(\Gamma)$ for $\delta t = 2$, 4 and 6 ns for each of two bandwidths ($W = 20$ and 40 MHz). Not surprisingly, the sensitivity of performance to this parameter is greater at larger bandwidths. In the remainder of

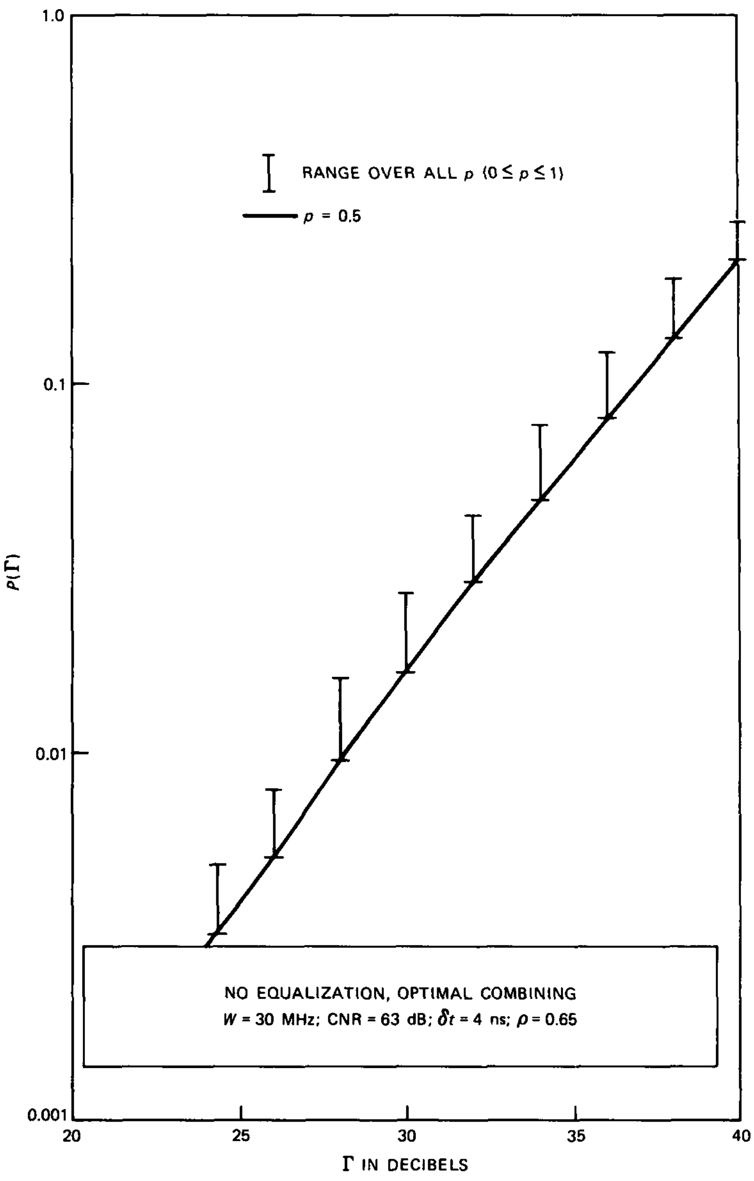

Fig. 5—Probability distributions for Γ in receivers with optimal diversity combining and no equalization. The vertical bars span the range from minimum to maximum over the p-range [0, 1.0] and the solid curve is for $p = 0.5$. Channel bandwidth $W = 30$ MHz and all other system and channel parameters have "typical" values.

this study, we will confine ourselves to the assumed "typical" value of 4 ns.

Figure 5 shows the effect of p, the minimum-phase probability, when $W = 30$ MHz. The vertical bars show the range of $P(\Gamma)$ as p goes from

0 to 1.0, and the solid curve is for the assumed "typical" value of 0.5. Similar results apply for other values of W. The highest point on each bar is for either $p = 0$ (all $H_1(f)$ and $H_2(f)$ minimum phase) or $p = 1.0$ (all $H_1(f)$ and $H_2(f)$ nonminimum phase), and the lowest point is for $p = 0.5$. The explanation for these trends is simple: The conditions $p = 0$ and $p = 1.0$ provide, on the average, for the greatest shape similarities between $H_1(f)$ and $H_2(f)$, while the condition $p = 0.5$ provides, on the average, for the greatest dissimilarities. In any event, Fig. 5 shows that a precise quantification of this parameter is not important for the situation under study.

We also examined the effect of the correlation factor ρ, for $W = 30$ MHz, over the range from 0 to 1.0 (we did not seriously consider anticorrelation). The spread was found to be very small, suggesting that the amplitude factors a_1 and a_2 in (4) are of minor import when CNR is high and that, therefore, the channel parameter ρ need not be precisely known. Clearly, then, poor performance occurs primarily when the relative variations of $H_1(f)$ and $H_2(f)$ are at once highly dispersive and (by random chance) highly similar. We invoked this observation to derive P_{req} in the Appendix.

5.3 Comparisons with non- and selection diversity

Figure 6 shows $P(\Gamma)$ for non-, selection, and optimal combining diversity without equalization. These comparisons are given for two bandwidths ($W = 20$ and 40 MHz). The parameters CNR, δt, p, and ρ are assigned their "typical" values. For non- and selection diversity, the values of δt and p have no influence on $P(\Gamma)$. The values of CNR and ρ were found to have some impact (the statistics improve slightly with increasing CNR for both non- and selection diversity, and improve slightly with decreasing ρ for selection diversity), but we did not study these relationships in detail.

For both bandwidths, receiver performance without space diversity or equalization is seen to be disastrous, as expected. Selection diversity improves matters noticeably, but is still far from adequate. The improvement in going to optimal combining diversity is seen to be dramatic.

5.4 Results for receivers with equalization

For receivers using ideal reciprocal equalizers, we have obtained both $P(\Gamma)$ and $P(R)$. We can thus examine trade-offs between detection performance (measured by $P(\Gamma)$) and dispersion at the equalizer input (measured by $P(R)$). For all diversity arrangements, both $P(\Gamma)$ and $P(R)$ depend weakly (if at all) on δt and p. In addition, $P(\Gamma)$ depends very weakly on W and $P(R)$ depends very weakly on CNR. In several cases, the correlation factor ρ was found to have a discernible

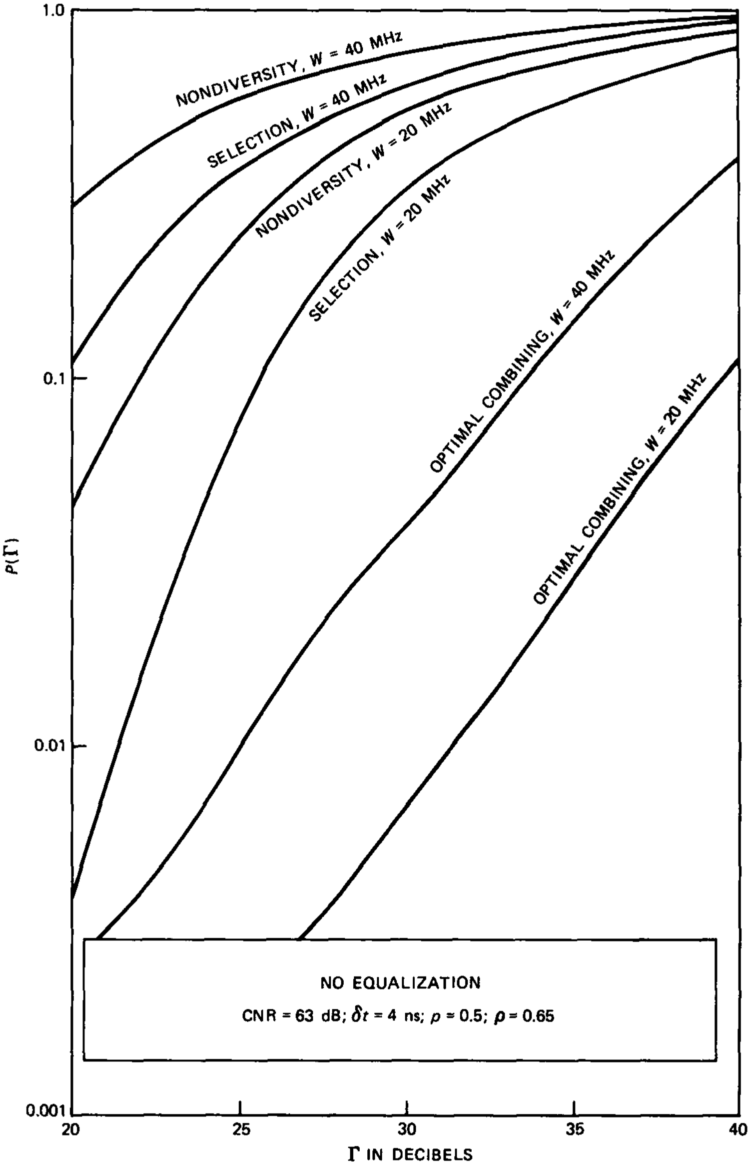

Fig. 6—Probability distributions for Γ in receivers with no equalization. Results are for non-, selection, and optimal combining diversity, for $W = 20$ and 40 MHz. All other system and channel parameters have "typical" values.

impact. This is because ideal equalizers tend to capitalize on total signal power and lower values of ρ (greater independence between a_1 and a_2) correspond to statistically higher values of total signal power. For this part of the study, we confined ourselves to the "typical" and somewhat conservative value of 0.65.

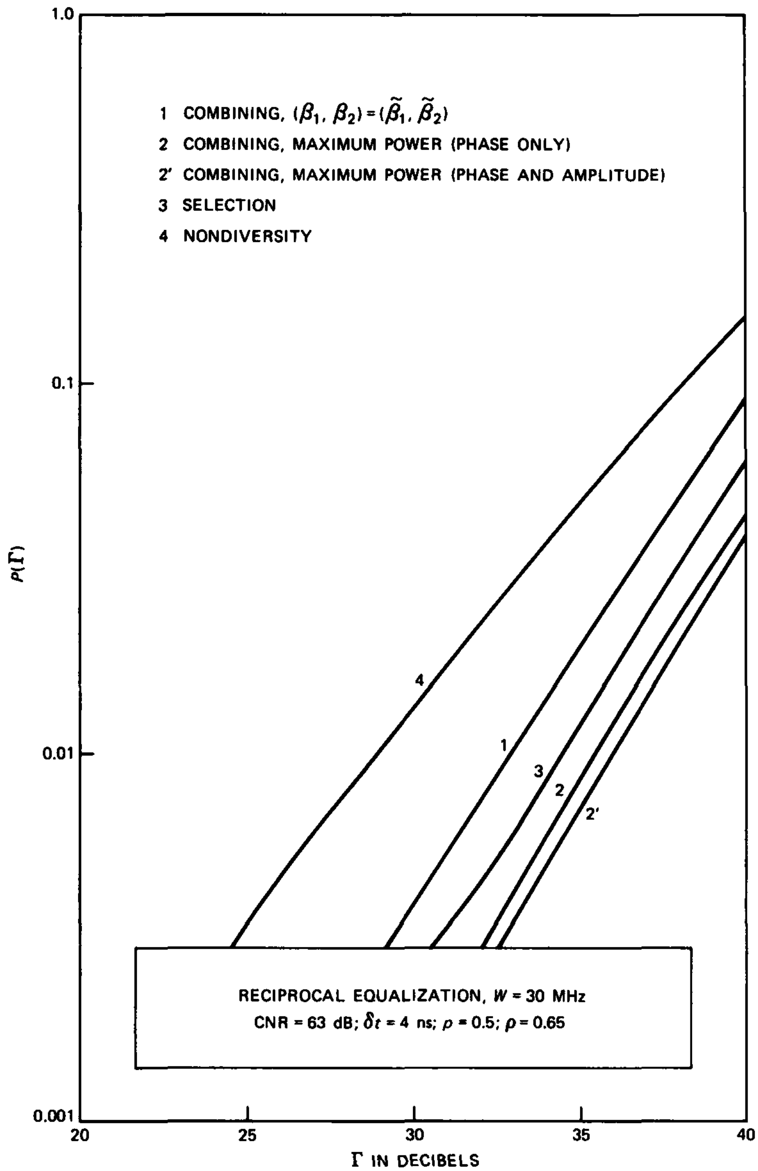

Fig. 7—Probability distributions for Γ in receivers with ideal reciprocal equalization. Results are for non-, selection, and combining diversity, with three gain-setting algorithms considered for the latter. Channel bandwidth $W = 30$ MHz and all other system and channel parameters have "typical" values.

5.4.1 Probability distributions for Γ

Figure 7 shows $P(\Gamma)$ for non-, selection and combining diversity, with three distinct gain-setting algorithms considered for the combining case. Some observations are as follows:

1. While the results shown are for $W = 30$ MHz, they would barely change for other bandwidths. With this in mind, we can see from Figs. 7 and 2 that a reciprocal equalizer alone would be less effective than an optimal diversity combiner alone for $W = 20$ MHz, but more effective for $W \geq 30$ MHz.

2. For reciprocal equalizers, Γ is related strictly to thermal noise enhancement. Thus, this quantity scales directly with CNR (63 dB in Fig. 7), that is, for every decibel of reduction (or increase) in CNR, all curves would shift by one decibel to the right (or left).

3. For combining diversity, the best results shown are for the (β_1, β_2) pairs that maximize combiner output power. Controlling both amplitude and phase is only slightly superior to controlling phase alone, which is only slightly superior to using selection diversity. Using the gain pair $(\tilde{\beta}_1, \tilde{\beta}_2)$, while optimal in the absence of equalization, is seen to be fourth best in this case. We now examine the potential benefit of using these suboptimal gains.

5.4.2 Probability distributions for R

Figure 8 shows $P(R)$ for $W = 20$ and 40 MHz. For each bandwidth, the results shown are for nondiversity, selection diversity, maximum-power combining diversity (phase-only adjustments), and "optimal" combining diversity, $(\beta_1, \beta_2) = (\tilde{\beta}_1, \tilde{\beta}_2)$. The disparities among approaches are seen to be strong, the best results corresponding to "optimal" combining.

VI. CONCLUSION

The results obtained in this study are subject to the usual uncertainties associated with finite simulations and a less-than-universal statistical model of dual-channel fading. Nevertheless, some general conclusions are possible, as follows:

1. The use of appropriate space diversity combining (e.g., the scheme described in Ref. 15) could eliminate the need in some links for post-combiner equalization.

2. In links where adaptive equalization *is* used, such a scheme could sharply reduce the signal dispersion at the equalizer input, thereby simplifying the equalizer design.

3. For purposes of assessing various receiver approaches, the dual-channel multipath fading model reported by Rummler is, for the most part, well specified. The precise value of the minimum-phase probability (p) appears to be of minor consequence, as is the precise value of the correlation factor (ρ) between the decibel values of a_1 and a_2. The delay parameter (δt) introduced here could have a modest impact if larger than 4 ns, particularly for the larger channel bandwidths.

4. Finally, the numerical results affirm that space diversity combin-

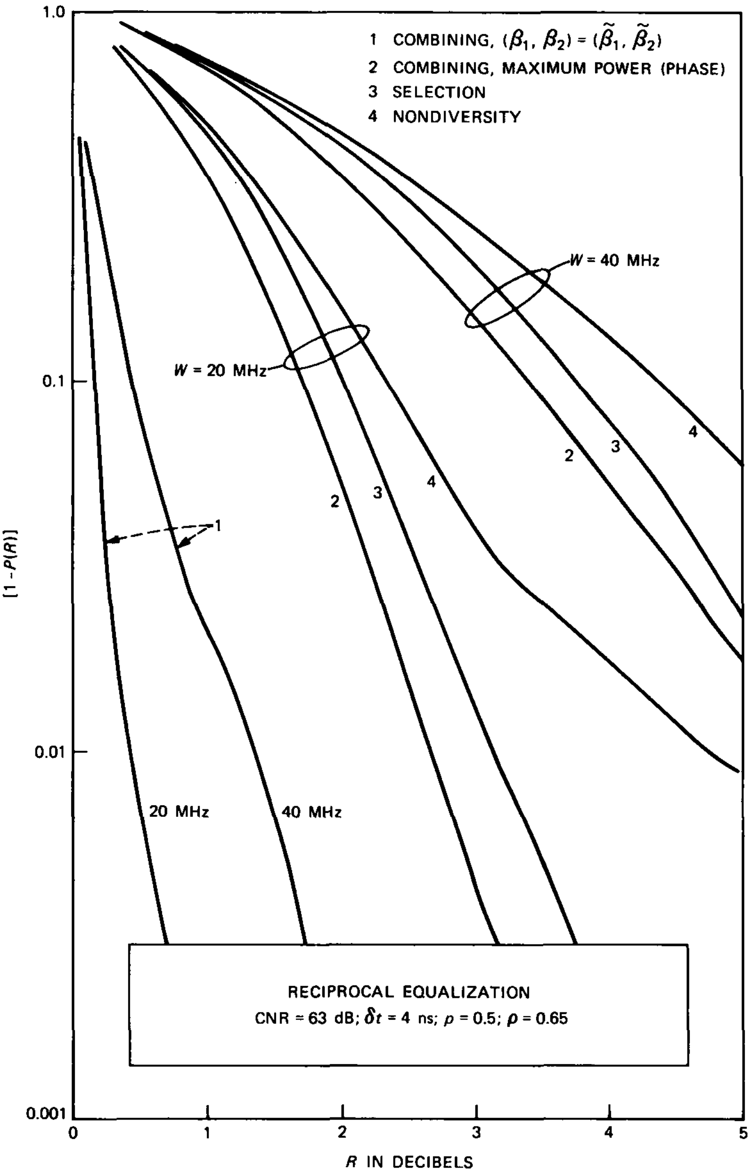

Fig. 8—Probability distributions for R for several diversity approaches, for $W = 20$ and 40 MHz. All other system and channel parameters have "typical" values.

ing and adaptive equalization in tandem comprise a formidable combination of receiver techniques in microwave digital radio.

VII. ACKNOWLEDGMENTS

Lisa J. (Domenico) Case made a major contribution to this study with her help in programming and executing the computer simulations. We are also grateful to Gerard J. Foschini for his valuable suggestions on methods of analysis.

REFERENCES

1. C. W. Anderson, S. G. Barber, and R. N. Patel, "The Effect of Selective Fading on Digital Radio," IEEE Trans. Commun., *COM-27*, No. 12 (December 1979), pp. 1870–5.
2. S. Komaki et al., "Characteristics of a High Capacity 16 QAM Digital Radio System in Multipath Fading," IEEE Trans. Commun., *COM-27*, No. 12 (December 1979), pp. 1854–61.
3. Y. Y. Wang, "Simulation and Measured Performance of a Space Diversity Combiner for 6 GHz Digital Radio," IEEE Trans. Commun., *COM-27*, No. 12 (December 1979), pp. 1896–907.
4. S. Komaki, Y. Okamoto, and K. Tajima, "Performance of 16-QAM Digital Radio System Using New Space Diversity," Paper 52.2, Int. Conf. Commun., June 8–12, 1980, Seattle, Washington.
5. T. Murase, K. Morita, and S. Komaki, "200 Mb/s 16-QAM Digital Radio System With New Countermeasure Techniques for Multipath Fading," Paper 46.1, Int. Conf. Commun., June 14–18, 1981, Denver, Colorado.
6. P. Hartmann and B. Bynum, "Design Consideration for an Extended Range Adaptive Equalizer," Paper 46.5, Int. Conf. Commun., June 14–18, 1981, Denver, Colorado.
7. A. J. Giger and W. T. Barnett, "Effects of Multipath Propagation on Digital Radio," IEEE Trans. Commun., *COM-29*, No. 9 (September 1981), pp. 1345–52.
8. P. D. Karabinis, "Maximum-Power and Amplitude-Equalizing Algorithms for Phase Control in Space Diversity Combining," B.S.T.J., *62*, No. 1, Part 1 (January 1983), pp. 63–89.
9. R. Iyer et al., "Effects of Space Diversity Reception on Multipath Induced Distortions in Terrestrial Microwave Channels," Paper 3.B.5, Int. Conf. Commun., June 13–17, 1982, Philadelphia, PA.
10. A. Ricagni and T. Testi, "IF Combining Techniques for Space Diversity in Analog and Digital Radio Systems," Paper 4.B.6, Int. Conf. Commun., June 13–17, 1982, Philadelphia, PA.
11. R. A. Nichols, "An IF Combiner for Digital and Analog Radio Systems," Paper 4.B.7, Int. Conf. Commun., June 13–17, 1982, Philadelphia, PA.
12. C. P. Bates and M. A. Skinner, "Impact of Technology on High Capacity Digital Radio Systems," Paper F2.3 Int. Conf. Commun., June 19–22, 1983, Boston, MA.
13. T. Noguchi et al., "6 GHZ 135 MBPS Digital Radio System With 64 QAM Modulation," Paper F2.4, Int. Conf. Commun., June 19–22, 1983, Boston, MA.
14. P. R. Hartmann and J. A. Crossett, "135 MBS-6 GHz Transmission System Using 64-QAM Modulation," Paper F2.6, Int. Conf. Commun., June 19–22, 1983, Boston, MA.
15. Y. S. Yeh and L. J. Greenstein, "A New Approach to Space Diversity Combining in Microwave Digital Radio," AT&T Tech. J., this issue.
16. W. D. Rummler, "A Statistical Model of Multipath Fading on a Space Diversity Radio Channel," B.S.T.J., *61*, No. 9, Part 1 (November 1982), pp. 2185–219.
17. W. D. Rummler, "A Rationalized Model for Space and Frequency Diversity Line-of-Sight Radio Channels," Paper E27, Int. Conf. Commun., June 19–22, 1983, Boston, MA.
18. W. D. Rummler, "A New Selective Fading Model: Application to Propagation Data," B.S.T.J., *58*, No. 7 (May–June 1979), pp. 1037–71.
19. W. D. Rummler, "More on the Multipath Fading Channel Model," IEEE Trans. Commun., *COM-29*, No. 3 (March 1981), pp. 346–52.
20. L. J. Greenstein and B. A. Czekaj, "A Polynomial Model for Multipath Fading Channel Responses," B.S.T.J., *59*, No. 7 (September 1980), pp. 1197–225.
21. R. W. Lucky, J. Salz, and E. J. Weldon, Jr., *Principles of Data Communication*, New York, NY: McGraw-Hill, 1968. (In particular, see pp. 50–51 for a description of cosine roll-off pulses and spectra.)
22. B. Widrow, "A Comparison of Adaptive Algorithms Based on the Methods of Steepest Descent and Random Search," IEEE Trans. Ant. and Prop., *AP-24*, No. 5 (September 1976), pp. 615–37.

23. R. W. Lucky, J. Salz, and E. J. Weldon, Jr., *Principles of Data Communication*, Chapter 6.
24. L. J. Greenstein and D. Vitello, "Digital Radio Receiver Responses for Combating Frequency-Selective Fading," IEEE Trans. Commun., *COM-27*, No. 4 (April 1979), pp. 671–81.
25. R. W. Lucky, J. Salz, and E. J. Weldon, Jr., *Principles of Data Communication*, Section 5.1.
26. P. Monsen, "Feedback Equalization for Fading Dispersive Channels," IEEE Trans. Inform. Theory, *IT-17* (January 1971), pp. 56–64.
27. M. S. Mueller and J. Salz, "A Unified Theory of Data-Aided Equalization," B.S.T.J., *60*, No. 9 (November 1981), pp. 2039–63.
28. G. J. Foschini and J. Salz, "Digital Communications Over Fading Radio Channels," B.S.T.J., *62*, No. 2, Part 1 (February 1983), pp. 429–56.
29. W. C. Wong and L. J. Greenstein, "Multipath Fading Models and Adaptive Equalizers in Microwave Digital Radio," IEEE Trans. Commun., *COM-32*, No. 8 (August 1984), pp. 928–34.
30. A. Gersho, "Adaptive Equalization of Highly Dispersive Channels for Data Transmission," B.S.T.J., *48*, No. 1 (January 1969), pp. 55–70.
31. N. Amitay and L. J. Greenstein, "Multipath Outage Performance of Digital Radio Receivers Using Finite-Tap Adaptive Equalizers," IEEE Trans. Commun., *COM-32*, No. 5 (May 1984), pp. 597–608.

APPENDIX

Derivation of P_{req}

We consider a specific W-Hz radio channel carrying digital traffic. It may be protected or unprotected and it may have dual space diversity or no diversity. Discernible multipath fading is assumed to exist, on one or both of the possible diversity branches, for T_o seconds per hop per year, with T_o given by (3). We define the following probabilities within that subset of time:

$P_o \triangleq$ The probability of outage per hop as experienced by a user of the channel;

$P_1 \triangleq$ The probability of outage per hop as experienced by the channel itself (note that $P_o < P_1$ when protection switching is used);

$P_{req} \triangleq$ The value of P_1 required to achieve a specified value of P_o.

We now make the following assumptions:

1. The yearly outage objective on a total system route is 0.005 percent (one way), apportioned uniformly among the route hops.

2. The path length and terrain factor for each hop are taken to have average values: $D = 25$ miles and $c = 1$ in (3).

3. Within any protection switching section, discernible multipath fading occurs on at most one hop at a time.

4. The subset of multipath fading seconds on each hop is congruent over all W-Hz channels within the same common carrier band.

5. Within that subset of multipath fading seconds, outage events are statistically independent from one W-Hz channel to another.

The third, fourth, and fifth assumptions are germane to calculations of P_{req} for systems with protection switching. The third assumption is slightly liberal, in that it leads to overestimation of P_{req}; the fourth assumption, by the same token, is somewhat conservative; and the fifth assumption is discussed later.

In systems without protection switching, P_o and P_1 are the same, and so P_{req} is just the value of P_o dictated by the first two assumptions. For a long-haul system (maximum length = 4000 miles), the outage budget will be met if each hop averages 10 seconds of outage per year; for a short-haul system (maximum length = 250 miles), that number is 160 seconds. Dividing each number by T_o yields the required P_{req}. The results are shown in Table II for the 4-, 6- and 11-GHz bands.

For systems *with* protection switching, the issue is more complicated, involving as it does the joint outage probabilities for channels within the same band. For most receiver techniques, outages in neighboring channels during multipath fading are *not* independent events, in which cases the fifth assumption cited above is too liberal. It might be quite valid, however, for the special case of optimal combining diversity without adaptive equalization. The reasoning is as follows: In such receivers, outage occurs primarily when $H_1(f)$ and $H_2(f)$ have similar shapes and, thus, dispersion cannot be reduced without excessive signal loss. There is no reason, however, why such a similarity between two uncorrelated responses would occur in *two* frequency channels at the same time, except by chance; hence, the independence assumption.

The case of optimal combining diversity without adaptive equalization is of major interest here, as we mean to explore the limits of its applicability in digital radio. Thus, we use the independence assumption in deriving P_{req}, speculating that the result is accurate for that type of receiver and somewhat elevated for most others.

To proceed, let N be the number of channels in a given band and assume that one of them is used for protection. Given an outage in a traffic-bearing channel, the probability that it will not find the protection channel available is

$$P_2 = P_1 + \binom{N-2}{2} P_1 + \text{smaller terms.}$$

The first term is the probability that the protection channel itself is out; the second term is the probability that the protection channel is *not* out but one of the other N-2 channels *is* and switches first; and the smaller terms (neglected here) have to do with three or more channels being out at the same time. Outage for a given user occurs if its original channel is out (probability P_1) *and* the protection channel is not available (probability P_2). Thus,

$$P_o = P_1 P_2 = \frac{N}{2} P_1^2.$$

We can now find the P_1 required to achieve a specified P_o. The latter values, as before, are $10/T_o$ and $160/T_o$, respectively, for long- and short-haul systems. The values of N are 12, 8, and 6, respectively, for the 4-, 6- and 11-GHz bands. The resulting values for P_{req} for each of various systems are shown in Table III.

AUTHORS

Larry J. Greenstein, B.S.E.E., 1958, M.S.E.E., 1961, and Ph.D. (Electrical Engineering), 1967, Illinois Institute of Technology; AT&T Bell Laboratories, 1970—. Mr. Greenstein currently heads the Radio Systems Research Department at Crawford Hill in Holmdel, NJ. His most recent work has dealt with communications satellites, mobile telephony, and microwave digital radio. His previous work was on digital encoding, digital filtering, and, at IIT Research Institute before 1970, airborne radar. Member, Eta Kappa Nu, Tau Beta Pi, and Sigma Xi; Senior Member, IEEE; Senior Technical Editor, IEEE Communications Magazine; co-recipient, IEEE Communications Society's 1984 Prize Paper Award in Communications Systems.

Yu-Shuan Yeh, B.S.E.E., 1961, National Taiwan University; M.S.E.E., 1964, Ph.D., 1966, University of California, Berkeley, CA; Harvard University, 1966–67; AT&T Bell Laboratories, 1967—. From 1961 to 1962, Mr. Yeh was an electronics officer in the Chinese Navy. He was a Research Fellow at Harvard University from 1966 to 1967 doing antenna research. In 1967 he joined AT&T Bell Laboratories and is currently a Supervisor in the Network Systems Research Department. His research interests include satellite communications, mobile radio, microwave digital radio, and data networks. Mr. Yeh holds over a dozen patents and is the recipient of two best paper awards from IEEE Transactions. Fellow, IEEE.